ARTICLE

New Observation of Na_2 $4^3\Sigma_g^+$ State by Pulsed Perturbation Facilitated Optical-Optical Double Resonance Spectroscopy

Zheng Chen[a], Cheng-zhe Cui[a], Yao-ming Liu[a], Li Li[a]*, V. B. Sovkov[b], V. S. Ivanov[b]

a. Department of Physics and Key Laboratory of Atomic and Molecular Nanosciences, Tsinghua University, Beijing 100084, China; b. V. A. Fock Institute of Physics, St. Pertersburg State University, Petrodvorets, St. Petersburg 198504, Russia

(Dated: Received on December 15, 2004; Accepted on April 26, 2005)

Sixty-five new vibronic levels of the Na_2 $4^3\Sigma_g^+$ state have been observed in the 33900−35200 cm^{-1} energy region above the potential minimum of the ground state by pulsed perturbation facilitated optical-optical double resonance (PFOODR) fluorescence excitation spectroscopy. These new data fill the gap between the low-v levels mainly observed by continuous wave (CW) PFOODR spectroscopy and the high-v levels above the 3s+3d limit observed by pulsed PFOODR with predissociation detection. Molecular constants are fitted below potential shelf around the 3s+3d atomic limit with previously published data (mainly observed by CW PFOODR) and these new data. RKR potential curve has been calculated with the new constants. The constants are: $T_e = 32127.090\ cm^{-1}$, $\omega_e = 121.4099(0.20720)\ cm^{-1}$, $B_e = 0.116287(0.0002300)\ cm^{-1}$, $R_e = 3.551$ Å. An error of the RKR potential curve of J. Chem. Phys. **108**, 7707 (1998) is corrected.

Key words: Na_2, Triplet states, PFOODR, $4^3\Sigma_g^+$ state, $3^3\Sigma_g^+$ state, Rydberg states

I. INTRODUCTION

The Na_2 $4^3\Sigma_g^+$ state, which dissociates adiabatically to the 3s+4p asymptote, was first observed by Li and Field using continuous wave (CW) perturbation facilitated optical-optical double resonance (PFOODR) fluorescence excitation spectroscopy [1]. More vibrational-rotational levels have been observed since then and hyperfine structure was resolved and analyzed [2–7]. The perturbations of the $4^3\Sigma_g^+$−$3^3\Pi_g^+$ and $4^3\Sigma_g^+$−$2^3\Pi_g$ states were observed and analyzed [4]. Vibrational levels of the $4^3\Sigma_g^+$ state above the 3s+3d atomic limit ($v \geq 28$) were observed to be strongly predissociated (accident predissociation by the $2^3\Pi_g$ state through the $3^3\Pi_g$ state) [5].

High quality *ab initio* calculations have characterized the lowest 84 electronic states of Na_2 up to the 3s+5p atomic limit, including the $4^3\Sigma_g^+$ state [8, 9].

Summarizing all the previous experimental works of the $4^3\Sigma_g^+$ state we found that the rovibronic levels of $v = 15-17, 20-26$ in the energy region of 33900−35200cm^{-1} had not been detected. In this article we present our new data in this energy region, molecular constants obtained with all available data, and the RKR potential energy curve.

II. EXPERIMENTAL

A Lambda Physik EMG 202MSE excimer laser simultaneously pumped two Lambda Physik FL3002E dye lasers, which were used as the *pump* and *probe* lasers. The two lasers counterpropagated and overlapped at the center of the heat pipe oven in which sodium vapor was generated. A Hamamatsu R212 photomultiplier tube (PMT) with UV-pass (maximum transmission was ∼50% at 320 nm) or violet-pass (maximum transmission was ∼20% at 430 nm) filters were used to detect UV fluorescence (from collision-populated $^1\Sigma_u^+/^1\Pi_u$ states to the $X^1\Sigma_g^+$ state) or violet fluorescence from the upper triplet states to the $a^3\Pi_u$ state (also to the lower vibrational levels of the $b^3\Pi_u$ state).

The pump laser was always operated with an intracavity etalon with linewidth 0.04 cm^{-1} and its frequency was calibrated by I_2 laser induced fluorescence (LIF). The probe laser was operated without an intracavity etalon (0.2 cm^{-1} linewidth) for a large region survey or with an etalon (0.04 cm^{-1} linewidth) for high resolution scans.

Figure 1 gives the PFOODR excitation diagram into the $^3\Sigma_g^+$ Rydberg states. The pump laser frequency was fixed to excite a selected $A^1\Pi_u$−$b^3\Pi_{\Omega_u}, v', J' \longleftarrow X^1\Sigma_g^+, v'', J'' = J' + 1$(or $J'' = J' - 1$) transition and the probe laser was scanned and the OODR excitation transitions into triplet state were detected by monitoring filtered molecular fluorescence with the PMT. The output of the PMT was sent to a Boxcar Averager and the OODR excitation signals were recorded by a computer.

III. RESULTS

Many $A^1\Sigma_u^+$−$b^3\Pi_u$ mixed levels of Na_2 have been identified. The intermediate levels we used in this experiment are the $b^3\Pi_{0u}$, v'=14 (perturbed by the $A^1\Sigma_u^+, v'$=8 level) J'=8, 10, 12, 14, $b^3\Pi_{0u}, v'$=13 (perturbed by the $A^1\Sigma_u^+$, v'=7 level), J'=31, and $b^3\Pi_{1u}, v'$=13, J'=26 levels [10–12].

More than 100 transitions into the $4^3\Sigma_g^+, v = 15-27$ vibrational levels have been identified in our spectra. Table I lists the intermediate levels, probe laser fre-

*Author to whom correspondence should be addressed. E-mail: lili@mail.tsinghua.edu.cn.

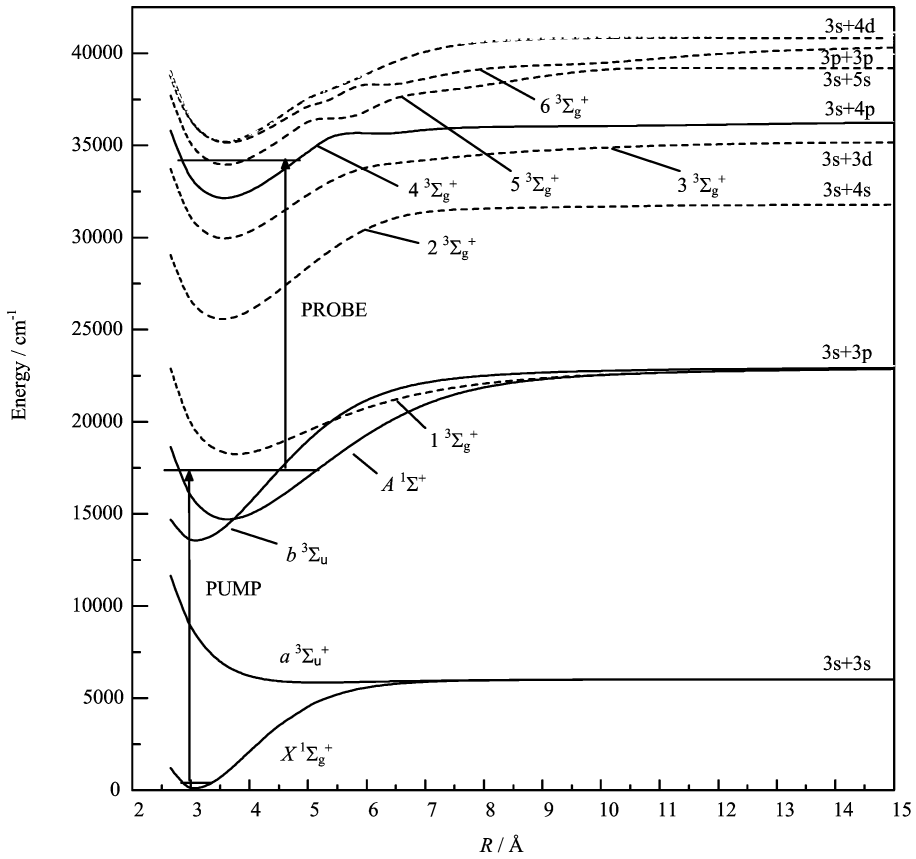

FIG. 1 PFOODR excitation diagram into Rydberg triplet states. Only the potential energy curves of the $^3\Sigma_g^+$ states are given in the diagram.

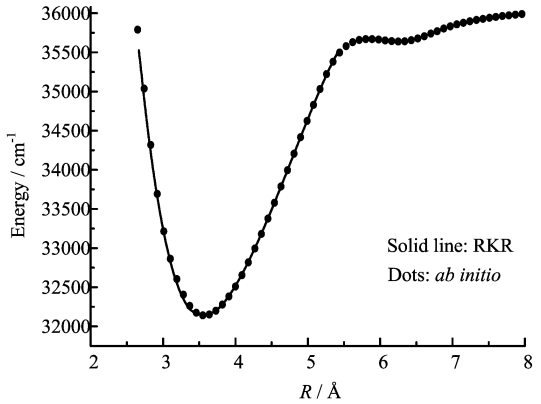

FIG. 2 RKR potential curve (solid line) and *ab initio* curve (dots) of Ref [1].

quencies, the $4^3\Sigma_g^+(v, N)$ assignments, and PFOODR term values of the newly observed $4^3\Sigma_g^+$ levels. Adding these new data, the data field nearly covers the whole potential energy curve of the $4^3\Sigma_g^+$ state.

The $4^3\Sigma_g^+$ has been known to have a potential shelf in the energy region above the 3s+3d atomic limit. We used all the available data below the shelf (slightly above the 3s+3d asymptote, up to v=31) to fit the Dunham constants and give the constants in Table II. Table II also gives previous constants for comparison.

Reference [5] reported the potential curve calculated from the G_v and B_v of v=0∼26 levels with the molecular constants of Ref. [4]. We found that the turning points for the low-v levels (especially the v = 0 level) given in Table II of Ref. [5] disagree with the turning points of the RKR curve calculated with molecular constants of Ref. [4]. Table III gives the RKR potential curve calculated with the new constants of Table II of the current paper. Figure 2 gives the RKR and *ab initio* potential curves. The agreement is very good.

So far the 2,3,4,6$^3\Sigma_g^+$ states of Na_2 have been observed [13–15]. These four $^3\Sigma_g^+$ states are core-penetrating Rydberg states: the $2^3\Sigma_g^+$ and $4^3\Sigma_g^+$, and $6^3\Sigma_g^+$ states are the nd (n=3, 4, 5) members, respectively, while the $3^3\Sigma_g^+$ state is the ns (n=4) member [16]. The ns (n=5) $^3\Sigma_g^+$ state, $5^3\Sigma_g^+$, has not been observed.

IV. ACKNOWLEDGMENT

This work was supported by the National Natural Science Foundation of China(NSFC No. 20473042, NO. 20173029 and 10174042), NKBRSF, and SRFDP of China and by RFBR(grant 05-03-39012) of Russia.

TABLE I Levels of the Na_2 $4^3\Sigma_g^+$ state observed

$A^1\Sigma_u^+ \sim b^3\Pi_u$		Frequency/cm^{-1}	$4^3\Sigma_g^+$		Term value/cm^{-1}	$A^1\Sigma_u^+ \sim b^3\Pi_u$		Frequency/ cm^{-1}	$4^3\Sigma_g^+$		Term value/cm^{-1}
v'	J'		v	N		v'	J'		v	N	
14	10	18261.121	15	9	33926.648	14	8	19106.145	23	7	34764.441
14	10	18265.577	15	11	33931.104	14	8	19109.512	23	9	34767.808
14	14	18257.555	15	13	33936.285	14	10	19102.339	23	9	34767.866
14	14	18263.648	15	15	33942.378	14	10	19106.522	23	11	34772.049
14	10	18369.421	16	9	34034.948	14	12	19100.533	23	11	34772.038
14	10	18373.801	16	11	34039.328	14	12	19105.489	23	13	34776.994
14	14	18365.754	16	13	34044.484	14	14	19098.263	23	13	34776.993
14	14	18371.744	16	15	34050.474	14	14	19104.018	23	15	34782.748
13	31	18475.654	16	30	34122.592	14	8	19206.951	24	7	34865.247
13	31	18488.359	16	32	34135.297	14	8	19210.329	24	9	34868.625
14	10	18477.024	17	9	34142.551	14	14	19204.741	24	15	34883.471
14	10	18481.061	17	11	34146.588	13	31	19305.472	24	30	34952.41
13	26	18584.814	17	25	34201.072	14	14	19304.429	25	15	34983.159
13	26	18595.566	17	27	34211.824	13	26	19407.417	25	25	35023.675
14	10	18793.642	20	9	34459.169	13	26	19417.885	25	27	35034.143
14	10	18797.921	20	11	34463.448	13	31	19404.242	25	30	35051.180
13	26	18900.450	20	25	34516.708	13	31	19416.587	25	32	35063.525
13	26	18911.174	20	27	34527.432	14	14	19397.313	26	13	35076.043
14	10	18897.639	21	9	34563.166	14	14	19403.006	26	15	35081.736
14	10	18902.010	21	11	34567.537	13	26	19505.441	26	25	35121.699
13	26	19003.506	21	25	34619.764	13	26	19515.702	26	27	35131.960
13	26	19014.196	21	27	34630.454	13	31	19501.902	26	30	35148.840
14	8	19004.174	22	7	34662.47	13	31	19514.348	26	32	35161.286
14	8	19007.634	22	9	34665.93	14	8	19502.800	27	7	35161.096
14	10	19000.441	22	9	34665.968	14	8	19506.058	27	9	35164.354
14	10	19004.692	22	11	34670.219	14	10	19498.896	27	9	35164.423
14	12	18998.636	22	11	34670.141	14	10	19502.992	27	11	35168.519
14	14	18996.485	22	13	34675.215	14	12	19497.010	27	11	35168.515
14	14	19002.294	22	15	34681.024	14	12	19501.805	27	13	35173.310
13	26	19106.389	22	25	34722.647	14	14	19494.552	27	13	35173.282
13	26	19116.529	22	27	34732.787	14	14	19500.200	27	15	35178.930

TABLE II Comparison of experimental molecular constants of the Na_2 $4^3\Sigma_g^+$ state (All units are in cm^{-1} except R_e which is in Å).

	Li *et al.* [4]	Whang *et al.* [3]	This work
T_e	32127.061(169)	32126.53(18)	32127.090(0.28)[a]
Y_{10}	122.322(69)	122.463(44)	121.4099246738456(0.20716934)
Y_{20}	−0.4567(97)	−0.4914(64)	−0.05786786154175161(0.066921276)
Y_{30}	$0.106(40)\times10^{-2}$	$0.431(35)\times10^{-2}$	−0.06827487463873894(0.01005859)
Y_{40}		$-9.94(64)\times10^{-5}$	$6.047759612969994(0.78828808)\times10^{-3}$
Y_{50}			$-2.799381012258961(0.33413609)\times10^{-4}$
Y_{60}			$6.546958185357516\ (0.72534233)\times10^{-7}$
Y_{70}			$-6.173448937527015(0.63134863)\times10^{-8}$
Y_{01}	0.11500(38)	0.11618(24)	0.1162873518300335(0.00023017541)
Y_{11}	$-0.611(29)\times10^{-3}$	$-0.699(30)\times10^{-3}$	$-8.710239424603028(0.62488539)\times10^{-4}$
Y_{21}		$0.20(12)\times10^{-5}$	$1.772330895942822(0.48336516)\times10^{-5}$
Y_{31}			$-4.078847259892586(1.0822773)\times10^{-7}$
Y_{02}		$-0.545(53)\times10^{-6}$[a]	-4.2672595×10^{-7} (calculated and fixed in the fit)[b]
R_e	3.571	3.5528	3.551[c]

[a] $T_e = Y_{0,0} - Y_{00}$, $Y_{00} = -0.1398\ cm^{-1}$; [b] Calculated from $Y_{02} = -4{Y_{01}}^3/{Y_{10}}^2$; [c] Calculated from $Y_{01} = B_e = h/(8\pi^2 c\mu R_e^2)$

TABLE III RKR potential curve

$R_{\min}$/Å	$R_{\max}$/Å	E/cm^{-1}	v	$R_{\min}$/Å	$R_{\max}$/Å	E/cm^{-1}	v
2.66361112989	5.43229831523	35528.8592923	31	2.95269605438	4.49234392532	33474.9245968	11
2.67560883879	5.37800018703	35438.7917882	30	2.97471475489	4.44130370271	33362.3049047	10
2.68700604968	5.32692070755	35346.2911816	29	2.99817164989	4.38877132354	33248.8438764	9
2.69814955458	5.27807473579	35251.8223106	28	3.02330710512	4.33447294042	33134.5235886	8
2.70928839059	5.23075977798	35155.7232392	27	3.05043334246	4.27806735728	33019.3206773	7
2.72060023779	5.18447370353	35058.2330498	26	3.0799720463	4.21910769612	32903.2101727	6
2.73220998305	5.13885872188	34959.5154812	25	3.11252107562	4.15697325422	32786.1714021	5
2.74420373585	5.09366082644	34859.6787245	24	3.14898136195	4.09074026641	32668.1962742	4
2.75663978841	5.04869953227	34758.7916872	23	3.19082312973	4.01891242338	32549.3002537	3
2.76955757969	5.00384445745	34656.8970371	22	3.2145193137	3.98013311114	32489.5215558	2.5
2.78298498183	4.95899736034	34554.0213376	21	3.22726935416	3.95981681069	32459.5539064	2.25
2.79694443783	4.91407800903	34450.1825839	20	3.24073678904	3.93876567355	32429.5363391	2
2.81145798488	4.86901347743	34345.3954531	19	3.25503697087	3.91686352538	32399.4709001	1.75
2.82655128794	4.82373032627	34239.6745784	18	3.27031873078	3.89396063973	32369.359929	1.5
2.84225707867	4.77814866867	34133.0361589	17	3.28677963364	3.86985846643	32339.2060817	1.25
2.85861777216	4.73217843131	34025.4982150	16	3.30469142673	3.84428418189	32309.012354	1
2.87568786844	4.68571651743	33917.0798031	15	3.32444574674	3.81684496913	32278.7821062	0.75
2.89353598663	4.63864514689	33807.7994974	14	3.34664398925	3.78693813969	32248.5190891	0.5
2.91224704304	4.59083042940	33697.6734530	13	3.37229850383	3.75354992770	32218.2274705	0.25
2.93192493005	4.54212065779	33586.7133595	12	3.4033818381	3.71470623471	32187.9118632	0

[1] L. Li and R. W. Field, J. Mol. Spectrosc. **117**, 245 (1986).
[2] L. Li, Q. Zhu and R. W. Field, Mol. Phys. **66**, 685 (1989).
[3] T. Whang, W. C. Stwalley, L. Li and A. M. Lyyra, J. Mol. Spectrosc. **157**, 544 (1993).
[4] L. Li and M. Li, J. Mol. Spectrosc. **173**, 25 (1995).
[5] J. Li, Y. Liu, H. Chen, H. Gao, J. Xiang, D. Chen, G. Wu, L. Li and R. W. Field, Chem. Phys. **108**, 7707 (1998).
[6] K. Tsai and T. J. Whang, Chin. Chem. Soc. **45**, 23 (1998).
[7] Y. Liu, L. Li, G. Lazarov, A. Lazoudis, A. M. Lyyra and R. W. Field, J. Chem. Phys. **121**, 5821 (2004).
[8] G. H. Jeung, Phys. Rev. A **35**, 26 (1987).
[9] S. Magnier, P. Millie, O. Dulieu and F. Masnou-Seeuws, J. Chem. Phys. **98**, 7113 (1994).
[10] H. Kato, M. Otani and M. Baba, J. Chem. Phys. **89**, 653 (1988).
[11] K. Shimizu and F. Shimisu, J. Chem. Phys. **78**, 1126 (1983).
[12] J. Shang and L. Li, private communication.
[13] T. Whang, C. Tsai, W. C. Stwalley, A. M. Lyyra and L. Li, J. Mol. Spectrosc. **160**, 411 (1993).
[14] T. Whang, W. C. Stwalley, L. Li and A. M. Lyyra, J. Mol. Spectrosc. **155**, 184 (1992).
[15] P. Yi, X. Dai, J. Li, Y. Liu, L. Li, V. B. Sovkov and V. S. Ivanov, J. Mol. Spectrosc. **225**, 33 (2004).
[16] J. Li, Y. Liu, X. Dai, L. Li and R. W. Field, Chem. Phys. **114**, 7859 (2001).